Cyclotron Absorption in Metallic Bismuth and Its Alloys

J. K. GALT, W. A. YAGER, F. R. MERRITT, AND B. B. CETLIN, *Bell Telephone Laboratories, Murray Hill, New Jersey*

AND

A. D. BRAILSFORD,* *Ford Motor Company, Dearborn, Michigan*

(Received January 21, 1959)

Extensive studies of cyclotron absorption in bismuth and in alloys of bismuth with tin and tellurium are reported. Experimentally, a microwave cavity arrangement is used which causes circularly polarized radiation to be incident on the sample. The samples are disks which form part of the cavity wall during the experiment. A signal is observed which is under most conditions proportional to the change in the fractional power absorption of the sample as the magnetic field applied to the sample is changed. The experiment is done with this field in the plane of the sample as well as normal to it. When the magnetic field is normal to the sample surface, circularly polarized radiation distinguishes between the effects of holes and of electrons. Making this distinction is complicated in bismuth by the anisotropy of the band structure, but it is not impossible. In pure bismuth the number of holes equals the number of electrons; alloying with tin increases the relative number of holes and alloying with tellurium increases the relative number of electrons. The experiments have been done both at 24 000 Mc/sec and at 72 000 Mc/sec. The tilted ellipsoid model of the electron band, and the ellipsoid of revolution model for the hole band have been used in a classical magneto-ionic theory of the effect which fits the data taken with magnetic field normal to the sample surface quite satisfactorily. The fit between this theory and the experiment is substantial confirmation of the validity of this band model, and makes it possible with the aid of certain infrared observations to determine the parameters of the model numerically. The mass parameters obtained for an ellipsoid in the electron band are $m_1=0.0088$, $m_2=1.80$, $m_3=0.02323$, $m_4=\pm 0.16$, while those for the hole band are $M_1=M_2=0.068$ and $M_3=0.92$. Comparison is made with similar results obtained from magnetoresistance and de Haas-van Alphen experiments. The experiments done with the magnetic field in the plane of the sample have been used to improve the accuracy of the determination of cyclotron resonance fields and therefore of the masses of the charge carriers, although no quantitative theory of the over-all shape of the signal under these conditions is available.

I. INTRODUCTION

As a means of studying their band structure, we have investigated cyclotron absorption in bismuth and some of its alloys. We have worked with bismuth because, while it has free charge carriers at absolute zero and is therefore metallic, the cyclotron absorption effect is large and easily observed in it. This happens because of the high mobility and relatively small number of the free charge carriers in this particular metal.

The classical description of cyclotron absorption is based upon the equation of motion for a free charge carrier in the presence of electric and magnetic fields, namely:

$$m d\mathbf{v}/dt = e(\mathbf{E}+\mathbf{v}\times\mathbf{B}) - m\mathbf{v}/\tau, \quad (1)$$

in rationalized mks units. Here $\mathbf{E}$ and $\mathbf{B}$ are the electric and magnetic fields, respectively, and $\mathbf{v}$ is the velocity of a charge carrier of charge and mass m scattered with relaxation time τ. The solution of this equation when the charge is subject to a steady applied magnetic field B_z and a small circularly polarized alternating electric field ($E_y=E_{y0}e^{j\omega t}=jE_x$) at right angles to it shows that the conductivity associated with the charge carrier in these fields has a resonance. This resonance occurs at a frequency given by:

$$\omega_c = \pm |e| B_z/m. \quad (2)$$

The magnetic field is assumed to lie along the z axis and is positive when in the plus z direction, negative when in the minus z direction. The sign of the magnetic field at resonance is determined by the sign of the charge e and by whether the polarization of the electric field is right or left circular with respect to the direction of the positive z axis. If a group of charge carriers is observed, Eq. (1) can be written in terms of average velocities, and the resonance occurs in the conductivity of the whole group.

We are concerned with the observation of the effect of this resonance on the behavior of the free charge carriers in solids at microwave frequencies. Early suggestions of the existence of such an effect[1–3] were followed by experimental discovery of the effect in a semiconductor, germanium.[4,5] Extensive observations of the effect in semiconductors have now been made.[6–13] Most of the theoretical work on this subject has assumed the validity of the effective mass approximation, and leads to the conclusion that the denominator in Eq. (2) is an effective mass, or a suitable combination of the

* Formerly Bell Telephone Laboratories, Murray Hill, New Jersey.

[1] J. Dorfmann, Doklady Akad. Nauk S.S.S.R. **81**, 765 (1951).
[2] R. B. Dingle, *Proceedings of the International Conference on Very Low Temperatures*, edited by R. Bowers (Oxford University Press, Oxford, 1951); Proc. Roy. Soc. (London) **A212**, 38 (1952).
[3] W. Shockley, Phys. Rev. **90**, 491 (1953).
[4] Dresselhaus, Kip, and Kittel, Phys. Rev. **92**, 827 (1953).
[5] Lax, Zeiger, Dexter, and Rosenblum, Phys. Rev. **93**, 1418 (1954).
[6] Dresselhaus, Kip, and Kittel, Phys. Rev. **95**, 568 (1954); **98**, 368 (1955).
[7] Dexter, Zeiger, and Lax, Phys. Rev. **95**, 557 (1954); **104**, 637 (1956).
[8] Fletcher, Yager, and Merritt, Phys. Rev. **100**, 747 (1955).
[9] Dresselhaus, Kip, Kittel, and Wagoner, Phys. Rev. **98**, 556 (1955).
[10] Burstein, Picus, and Gebbie, Phys. Rev. **103**, 825 (1956).
[11] Keyes, Zwerdling, Foner, Kolm, and Lax, Phys. Rev. **104**, 1805 (1956).
[12] W. S. Boyle and A. D. Brailsford, Phys. Rev. **107**, 903 (1957).
[13] B. Lax, Revs. Modern Phys. **30**, 122 (1958).

tensor components of the effective mass.[3] Our results strongly support the validity of this assumption in bismuth. More complicated cases have been studied by Luttinger and Kohn,[14] and others.[15,16] We will content ourselves here with the remark that a more general form of Eq. (2) may be derived[17] following Shockley.[18]

Cyclotron resonance experiments are done on semiconductors by placing a sample in a microwave cavity. The alternating E field is supplied by the microwave fields inside the cavity, and the whole cavity is between the poles of an electromagnet with which a steady B_z field is applied. The sample only perturbs the microwave fields slightly in this experiment; hence their shape is that of the fields in the empty cavity, and they remain constant during the experiment, in first approximation. The power absorbed per unit volume is $P_{\text{abs}}=\sigma E^2$, and since the conductivity σ has a resonant maximum when the cyclotron resonance condition [Eq. (2)] is satisfied, a resonance absorption line is observed at this point. The relaxation time, τ, for the charge carriers is long, especially at low temperatures in the semiconductors studied in this way, and this line is therefore narrow and well resolved.

Several added experimental difficulties arise when we undertake to do this experiment on metals. In the first place, the depolarizing fields which build up as a result of any motion of a charge cloud as dense as those in metals would in general prevent significant amounts of motion of the sort involved in cyclotron resonance. This problem has been discussed by Dresselhaus, Kip, and Kittel[19]; another way of stating it is to point out that while the microwave experimental frequencies are well *above* the plasma frequencies of the charge carriers in most semiconductor samples, they are in general *below* the plasma frequencies of the charge carriers in a metal sample. In the second place, at microwave frequencies in metals one is often in the region of the anomalous skin effect,[20] where the mean free path of the charge carriers is large compared to the skin depth and a charge carrier moves a distance larger than a skin depth in a period of the electromagnetic field. This effect makes the surface impedance of a metal less dependent on steady magnetic fields applied normal to the surface. In fact, in the extreme anomalous limit, the surface impedance is substantially independent of a magnetic field applied in this way.[21–23] Less important difficulties are that in metals relaxation times are in general shorter, and the resolution of the experiment poorer, and that skin depths are so small in metals that unless sample dimensions and orientations are chosen carefully the microwave field would not be uniform in a sample placed inside the cavity.

These new problems introduced by the peculiarities of metals as opposed to semiconductors are not insuperable, however. Metals differ from semiconductors in that the charge carriers cause the conductivity and effective dielectric constant to be very high compared to that of the lattice alone. Consequently a metal sample may be used to form part of the cavity wall and thus be examined by reflecting radiation from it; this in fact is the arrangement used in the present experiments. The most important result of this arrangement is that there are no depolarizing fields inside the sample; the free charge as it moves drains off the end of the sample. In other words, while the plasma frequencies of the charge carriers in the sample are high in general, the one in this sample relevant to the motion associated with cyclotron resonance is zero. The difficulty with depolarizing fields is therefore overcome. Furthermore, while the skin effect now enters the experiment, it does so in such a way that account can be taken of it in analyzing the experiment. As for the problem of short relaxation times, experimental frequencies of 24 000 Mc/sec and 72 000 Mc/sec are high enough to gain most of the important information from experiments of this sort on bismuth.

The relation of the anomalous skin effect to these experiments is discussed quantitatively in Appendix B. Under the conditions used in these experiments, the samples are often near, but only rarely in the anomalous region. When anomalous conditions do occur in a sample, they occupy only a small fraction of the magnetic field range. As a result, while the effect is relevant to bismuth in general, it is not a vital factor in these experiments. Azbel' and Kaner,[23] however, have suggested that cyclotron resonance experiments can be done even under extreme anomalous conditions when the steady magnetic field is in the plane of the metal. Significant effects have been observed under these conditions[24] in other metals; Aubrey and Chambers[25] have seen and interpreted this effect in bismuth under more anomalous conditions than those in the experiments reported on here.

If some of the problems mentioned above are solved by making the sample part of the microwave cavity wall, however, the interpretation of the experiment requires more analysis than does the experiment on semiconductors. The sample no longer merely perturbs

[14] J. M. Luttinger and W. Kohn, Phys. Rev. **97**, 869 (1955).
[15] Zeiger, Lax, and Dexter, Phys. Rev. **105**, 495 (1957).
[16] J. M. Luttinger, Phys. Rev. **102**, 1030 (1956).
[17] I. M. Lifshits and A. M. Kosevich, Zhur. Eksptl. i Teoret. Fiz. **29**, 730 (1955) [translation: Soviet Phys. JETP **2**, 636 (1956)].
[18] W. Shockley, Phys. Rev. **79**, 191 (1950).
[19] Dresselhaus, Kip, and Kittel, Phys. Rev. **100**, 618 (1955).
[20] H. London, Proc. Roy. Soc. (London) **A176**, 522 (1940). A. B. Pippard, Proc. Roy. Soc. (London) **A191**, 370 (1947); **191**, 385 (1947). G. E. H. Reuter and E. H. Sondheimer, Proc. Roy. Soc. (London) **A195**, 336 (1948).
[21] R. G. Chambers, Phil. Mag. **1**, 459 (1956).
[22] M. Ia. Azbel' and M. I. Kaganov, Doklady Akad. Nauk S.S.S.R. **95**, 41 (1954).
[23] M. Ia. Azbel' and E. A. Kaner, Zhur. Eksptl. i Teoret. Fiz. **30**, 811 (1956) [translation: Soviet Phys. JETP **3**, 772 (1956)].
[24] E. Fawcett, Phys. Rev. **103**, 1582 (1956); Kip, Langenberg, Rosenblum, and Wagoner, Phys. Rev. **108**, 494 (1957); P. A. Bezuglyi and A. A. Galkin, Zhur. Eksptl. i Teoret. Fiz. **33**, 1076 (1957) [translation: Soviet Phys. JETP **6**, 831 (1958)]. Galt, Merritt, Yager, and Dail, Phys. Rev. Letters **2**, 292 (1959).
[25] J. E. Aubrey and R. G. Chambers, J. Phys. Chem. Solids **3**, 128 (1957).

the fields, but in fact largely determines their values in its own neighborhood. Consequently not only the conductivity, but related quantities such as skin depth, the magnitude of **E** in the sample, and the impedance mismatch across the surface of the sample are all dependent on B_z. The problem is essentially that of calculating, from Eq. (1) and Maxwell's equations, the absorption coefficient for a plane wave incident on a plane surface. This problem has been discussed at various places in the literature,[19,21,22,26,27] but Anderson[28] has given a treatment directly relevant to our experiments which has formed the basis of our interpretation of the data. The treatments given to date, however, either assume that the conductivity is isotropic in the plane normal to the magnetic field [see Eqs. (7) and (8)], or do not discuss the effect of anisotropy in this conductivity on the boundary problem. The interpretation of our data requires a complete treatment of this anisotropic problem. Furthermore, an understanding of the data requires, in addition to the theory of these references modified to take account of anisotropy, a recognition of the fact that when two carriers are present the real part of the dielectric constant of the metal may go through zero at points quite different from cyclotron resonance. The occurrence of this phenomenon is related to the plasma frequencies of the charge carriers[29,30]; it has not been emphasized previously. These points and the points where cyclotron resonance occurs will be referred to as "singularities" in our data.

Preliminary observations of cyclotron absorption in bismuth in experiments similar to ours have been made previously by some of us[31] and by Dexter and Lax.[27]

II. EXPERIMENTAL

Our experiments have been carried out using circularly polarized radiation.[6] This requires added care in our experimental arrangements, but it makes possible much higher resolving power than linear polarization. Furthermore, the microwave circuit arrangements which have been used achieve simultaneously both circular polarization of the radiation incident on the sample and a very sensitive response to the cyclotron absorption effect.

The geometry of the microwave experimental arrangement is shown in Fig. 1. The microwave signal passes the cavity as it travels along a wave guide which is bent into a U-shape so that it will fit into a suitable helium Dewar. The cavity is cylindrical in shape and

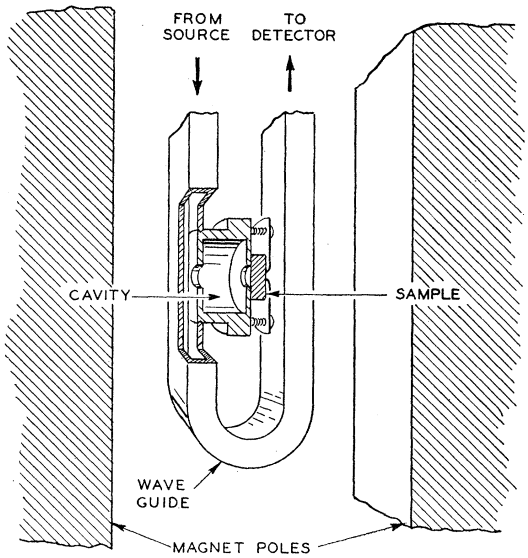

FIG. 1. Diagram of geometry of microwave arrangement used in studying cyclotron absorption in bismuth. Proper placement of cavity on the broad side of the wave guide and small additional adjustments cause the radiation incident on the sample to be circularly polarized.

is placed on the wave guide so that it can be excited by the field in the guide through a hole at one of its ends. It is excited in a TE_{112} mode at 24 000 Mc/sec and in a TE_{113} mode at 72 000 Mc/sec. In both these modes the **E** field is everywhere normal to the cavity axis, and the frequency is degenerate with respect to the direction of polarization of the **E** field pattern in the plane normal to the axis. The coupling hole at the end of the cavity is placed on the broad side of the wave guide but off center at such a point that the excitation causes the TE_{112}, or TE_{113} field pattern to rotate about the cavity axis at the microwave frequency. The radiation on the axis is thus circularly polarized, and since the sample covers a hole at the center of the end of the cavity opposite the coupling hole, it forms the wall of the cavity in an area where circularly polarized radiation is incident upon it. The polarization is only perfectly circular right on the cavity axis; consequently the sample diameter is not allowed to be more than 30% of the cavity diameter.

The achievement of circularly polarized radiation in this way depends on making the cavity perfectly degenerate. This requires careful attention to machining tolerances, but final realization of this condition also requires adjustments in the form of small cylindrical metal studs which can be moved in and out of the cavity on screw threads. Two of these studs have been used in the present experiments, each perpendicular to the other and to the cavity axis. Adjustment of one stud is possible even when the Dewar is in place and the cavity is at the experimental temperature.

The fact that circularly polarized radiation was incident on the sample was checked at 24 000 Mc/sec

[26] B. Donovan and E. H. Sondheimer, Proc. Phys. Soc. (London) **A66**, 823 (1953).
[27] R. N. Dexter and B. Lax, Phys. Rev. **100**, 1216 (1955); Lax, Button, Zeiger, and Roth, Phys. Rev. **102**, 715 (1956).
[28] P. W. Anderson, Phys. Rev. **100**, 749 (1955).
[29] H. Fröhlich and H. Pelzer, Proc. Phys. Soc. (London) **A68**, 525 (1955).
[30] P. Nozières and D. Pines, Phys. Rev. **109**, 762 (1958); **109**, 1062 (1958).
[31] Galt, Yager, Merritt, Cetlin, and Dail, Phys. Rev. **100**, 748 (1955).

by observations of paramagnetic resonance in a sample of calcium copper acetate hexahydrate. The sample was placed in the cavity at the outer rim of the bismuth while the cyclotron absorption experiment was conducted. Under these circumstances, the ratio of the intensities of the paramagnetic resonances observed when the steady magnetic field is in opposite directions then gives a minimum for the average circularity over the sample. This ratio was at least 10 in all experiments for which data is shown; in most of them it was 20 to 30. It should be emphasized that in observing these ratios care must be taken that power saturation of the paramagnetic resonance does not occur. This check on circularity was not made at 72 000 Mc/sec because of difficulty in finding a suitable paramagnetic material which had a resonance at sufficiently low magnetic fields. However, the data itself confirms the circularity of the radiation at this frequency, both by its asymmetry with respect to the direction of the applied magnetic field and by the fact that it fits the same theory as the 24 000 Mc/sec data.

The microwave arrangement shown in Fig. 1 not only applies circularly polarized radiation to the sample, but also has other features of some interest. These features arise from the following fact: when a wave travels down the guide and is incident on the cavity, it excites only one of the two possible circular polarizations in the cavity by virtue of the off-center position of the cavity on the broad side of the wave guide. Some of the energy which enters the cavity is absorbed and some is reradiated. The peculiar feature of this arrangement is that from reciprocity it is clear that the energy reradiated from the cavity all returns along the path of the incident radiation toward the source, and none goes toward the detector. This makes it possible to achieve most of the advantages of a microwave bridge by coupling the cavity closely to the wave guide and absorbing or reflecting most of the incident power at the cavity. If there is an element in the cavity which mixes the two circular polarizations of electromagnetic radiation, some of the reradiated power will travel to the detector, and the behavior described above is modified. Some of the samples reported on here have an anisotropic conductivity which tends to cause such mode mixing, but the amount of this mixing is small.

Microwave filter circuits with the features mentioned above have been discussed by Cohn and Coale.[32] The present arrangement will be discussed by means of an equivalent circuit similar to one of theirs, which is valid when the cavity is near resonance; the circuit is shown in Fig. 2. This circuit can be understood if the cavity oscillation producing circular polarization is thought of as synthesized from two modes polarized linearly at right angles to each other and excited 90° out of phase with one another. The power absorption coefficient of the sample is proportional to an additive contribution

[32] S. B. Cohn and F. S. Coale, Proc. I.R.E. 44, 1018 (1956).

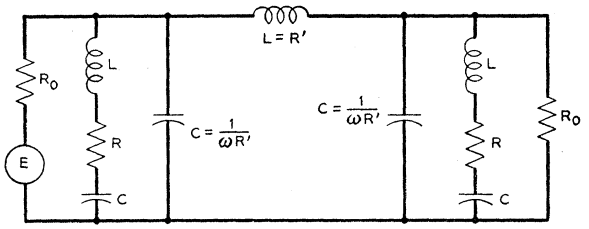

FIG. 2. Equivalent circuit of microwave cavity arrangement shown in Fig. 1. This circuit is only valid near a particular cavity resonance.

to R in this circuit. Note, however, that the values of the circuit impedances in Fig. 2 are those in the wave guide circuit, which is represented here by a two wire transmission line matched at both source and detector ends. Consequently, they include a factor determined by the coupling between the cavity and the wave guide. If this coupling is increased, the cavity impedances in Fig. 2 all decrease, and a larger fraction of the incident power enters the cavity, while a correspondingly smaller part is transmitted past the cavity to the detector. By increasing the coupling to very large values, the signal at the detector can be made very small. Under these conditions, a small change in the power absorbed by the cavity causes a relatively large fractional change in the signal at the detector, and we thus achieve the gain inherent in a bridge. The magnitude of the coupling between the cavity and the wave guide is determined by the Q of the cavity and by the size of the coupling hole in its end wall.

Quantitatively, a straightforward solution of the network equations for the circuit shown in Fig. 2 shows that when the cavity is at resonance the power dissipated in the load resistance is:

$$P_{\text{load res.}}=\tfrac{1}{2}(E^2/R_0)[\tfrac{1}{2}R/(R+R_0)]^2. \quad (3)$$

The voltage across the load at resonance, $V_{\text{L.R.}}$, is therefore:

$$V_{\text{L.R.}}=(E/\sqrt{2})[\tfrac{1}{2}R/(R+R_0)]. \quad (4)$$

From this it follows immediately that the fractional change in $V_{\text{L.R.}}$ as R changes is:

$$(1/V_{\text{L.R.}})(dV_{\text{L.R.}}/dR)=(R_0/R)[1/(R+R_0)]. \quad (5)$$

It is therefore clear that this fractional change becomes larger for the same change in R if the coupling is adjusted so that R is small.

At 24 000 Mc/sec double detection was used; consequently a signal was observed which was proportional to the change in the *voltage* across the load as the magnetic field varied from $B_z=0$ in either direction. At 72 000 Mc/sec single detection was used. This was shown experimentally to give a response proportional to the square of the incident voltage (voltage across the load). Consequently at this frequency a signal was observed which was proportional to the change in the *power* dissipated in the load as B_z varied. It can be

shown from Eqs. (3) and (4) that as R increases from a value small compared to R_0 (the condition at $B_z=0$) to the larger values which correspond to higher fields, the change in power dissipated in the load is a much more linear function of the change in R than is the change in voltage across the load. The data reflect this fact; at 24 000 Mc/sec they show saturation effects at high magnetic fields. However, these effects are not large enough to distort the data seriously, because the Q of the cavity used at 24 000 Mc/sec was lowered deliberately by plating one end of it with rhodium, thereby effectively increasing R_0. As the above remarks imply, since changes in B_z cause no change anywhere else in the system, we identify this variation in R with a change in the absorption coefficient of the sample. We therefore compare the observed signals with calculated power absorption coefficients in order to deduce the fundamental parameters which characterize conduction in bismuth.

At 24 000 Mc/sec a somewhat novel microwave bridge was used to improve sensitivity. Since the magnitude of the signals from bismuth was in most cases large this bridge was a convenience rather than a necessity, and it will be described only briefly. A current actuated ferrite isolator was placed in the wave guide after the cavity, and its current was square wave modulated at a frequency of 27 cps, with the result that the microwave signal was also square wave modulated off and on at this frequency. The detector then sees the signal in pulses of 27-cycle repetition rate whose length is such that they impinge on the crystal half the time. A dummy wave-guide arm is modulated with another isolator in the opposite phase to the signal arm and thereby provides a signal which impinges on the crystal the other half of the time. The dummy arm is adjusted so that at zero B_z the two signals are equal, and no 27-cps signal strikes the detector. As B_z is varied, R changes, the signal which passes the cavity changes, and the bridge is unbalanced, so a signal is observed at the detector which, however, is at 27 cps rather than dc. This makes it possible to use a lock-in amplifier and phase detector, thereby achieving very narrow signal bandwidth and correspondingly low noise levels. Another feature of this arrangement is that it is not sensitive to microwave phase balance in the bridge.

Magnetic field modulation techniques have also been used in the present work to observe the derivative of the signal as a function of B_z, but because of the broadness in B_z of the effects observed these data are in general less informative than those taken as described above and will therefore not be presented in this paper.

All data was taken continuously on a tape recorder as B_z was varied.

The crystal structure of bismuth is rhombohedral; the unit cell (not the primitive cell) is a slightly distorted cube, and one of the cube body diagonals is along the three-fold axis in the bismuth. Aside from this three-fold axis, there are two other nonequivalent principal directions in the crystal. One is a two-fold axis, of which there are three arranged at 120° angles with each other in the plane perpendicular to the three-fold axis. The other is a so-called bisectrix of which there are also three; they lie in the same plane as the two-fold axes, and bisect the angles between them.

The data have been taken with the magnetic field along principal axes in pure bismuth and in several alloys of it with small quantities of tin and tellurium. Pure bismuth has an equal number of holes and electrons as our data and that of others[33] show. Alloying with tin causes the number of holes to increase and the number of electrons to decrease; alloying with tellurium has the reverse effect. The data presented here show this effect, and thus confirm the earlier results of Thompson.[34]

The samples used in these experiments were prepared from bismuth purified by means of zone refining techniques. This bismuth was supplied to us by J. H. Wernick and K. H. Benson, and crystals were grown of it and of the various alloys by C. E. Miller; these crystals were in the form of cylindrical boules.

The crystals in boule form were oriented by x-ray techniques, and disks 3 or 4 mm thick were cut from each oriented boule with an acid string saw. The cutting acid was concentrated HNO_3, and the string was linen thread which only made one pass through the cut and was then thrown away. Two disks were cut from each boule, one normal to a three-fold axis, and one normal to a two-fold axis. In the case of pure bismuth, a disk was also cut normal to a bisectrix axis. Both sides of each disk were abraded flat with 2/0 emery paper while held in a jig which maintained sample orientation. The paper was lubricated with a mixture of 2 parts kerosene and one part machine oil. The strain left by this procedure was removed by etching about 0.04 cm off each side of the sample. This treatment left a surface such that visual examination of Laue spots on an x-ray photograph revealed no strain. The best etchant found for doing this while leaving the surfaces clean and flat was 3 parts H_2O+2 parts HNO_3+1 part HCl used at temperatures between 70 and 100°C. This treatment left a film, which was removed by a dip of about 5 sec in concentrated HNO_3 at room temperature. In some cases when the samples were placed on the microwave cavity, however, high spots in contact with the outside of the cavity wall removed from the area exposed to microwaves had to be filed down in order to obtain better contact at the edge of the hole which the sample covered. This was especially true in the 72 000 secc/M work.

III. RESULTS

The experimental results consist of plots (*vs* B_z) of a quantity which is proportional to the change of power

[33] B. Abeles and S. Meiboom, Phys. Rev. **101**, 544 (1956).
[34] N. Thompson, Proc. Roy. Soc. (London) **A155**, 111 (1936); **A164**, 24 (1938).

absorption coefficient of the sample as B_z varies from zero. Thus, the experiments do not determine the absolute value of the power absorption coefficient; however, our theoretical analysis[35] makes it possible to remedy this difficulty for data taken with the magnetic field perpendicular to the plane of the sample along either a two-fold or a three-fold axis. In the course of plotting, these data have been adjusted by comparison with the theoretical curves in scale and with respect to zero power absorption coefficient so that they are displayed in the figures as the absolute value of the power absorption coefficient; the remaining data are plotted on a relative basis. In the cases for which the complete theoretical analysis is quantitatively valid, theoretical curves are shown in the same figure with the data; these curves will be discussed in the next section. The data at 24 000 Mc/sec show saturation effects which reflect the nonlinearity in the relation between the signal and R at this frequency as discussed in Sec. II. The experimental curves are corrected for this effect in various ways as indicated in the figure captions.

Data are presented at both 24 000 Mc/sec and 72 000 Mc/sec with B_z perpendicular to the surface of the sample. Data were taken at both frequencies with B_z parallel to the sample surface also, but only those for 72 000 Mc/sec on pure bismuth are presented. The 24 000 Mc/sec data and the data taken in this way on alloys give no additional information and in fact do not

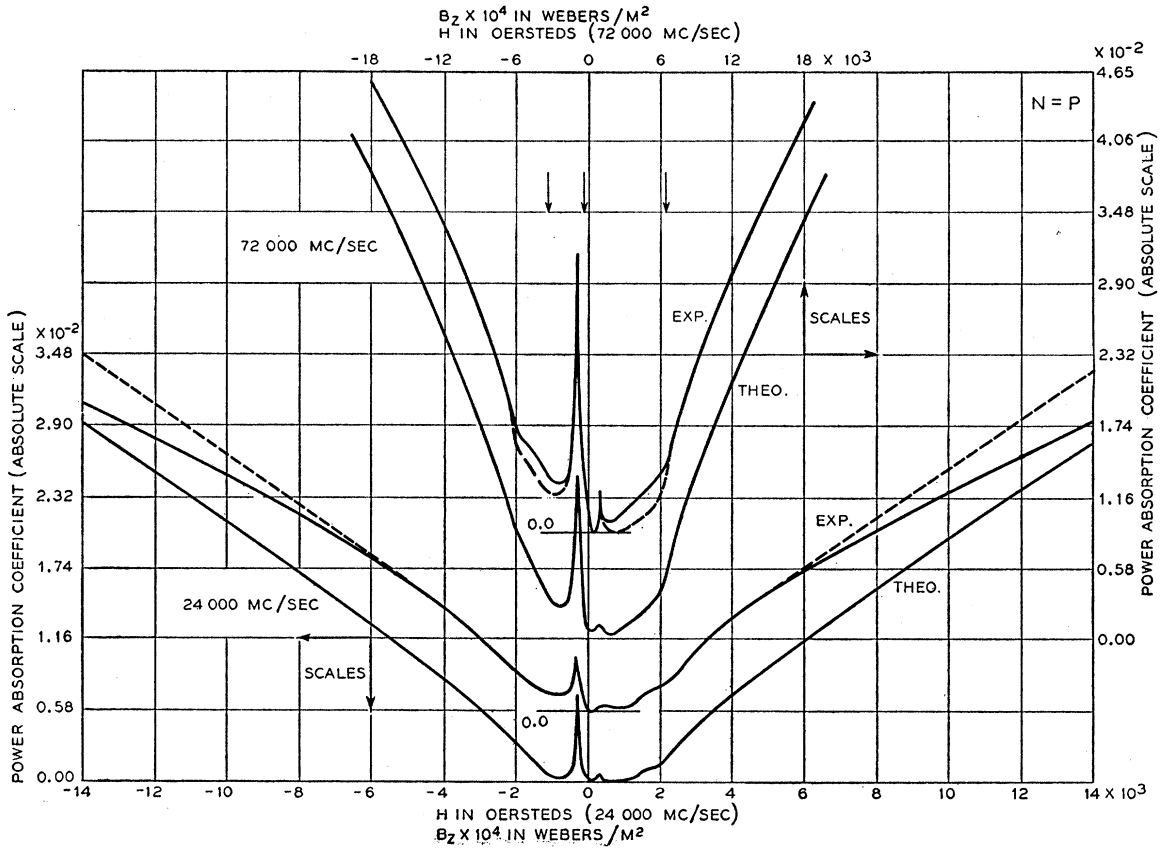

FIG. 3. Plots of power absorption coefficient *vs* magnetic field from both theory and experiment with magnetic field normal to sample surface and along a two-fold axis in pure bismuth. Curves for two frequencies are shown and the ordinate scales give absolute values. Zero absorptivity for the experimental curves is offset vertically from that for the theoretical curves, and its position is indicated on the vertical axis at zero field. The magnetic field scale used at 72 000 Mc/sec is compressed by a factor three with respect to that used at 24 000 Mc/sec so that the cyclotron field for a given set of carriers is on the same vertical line for all curves. Vertical arrows indicate these fields; there are two for electrons and one for holes. It will be noticed that the curves show effects at the fields indicated by these arrows on both sides of $B=0$. This is a result of the anisotropy of the bands in bismuth. The relaxation times used in calculating the theoretical curve at 72 000 Mc/sec are such that for holes $\omega\tau=30$ and for electrons $\omega\tau=3$. At 24 000 Mc/sec they were such that for holes $\omega\tau=20$ and for electrons $\omega\tau=10$. A lower $\omega\tau$ for electrons at 24 000 Mc/sec would make the theoretical curve fit the data better in the neighborhood of the peak at -300 oe, but the present value is used in order to display the anisotropy more clearly. At 72 000 Mc/sec the fit between experiment and theory would be improved if we used $\omega\tau\cong1$ for the higher mass electrons and $\omega\tau\cong10$ for those of lower mass, but our theoretical treatment assumed that the relaxation time for all electrons was the same. A dashed line shows how the experimental curve at 24 000 Mc/sec would look in the absence of the saturation which occurs in the experiments at that frequency. Another dashed line shows approximately how the 72 000 Mc/sec data would look in the absence of the reflected wave of the wrong circularity.

[35] Boyle, Brailsford, and Galt, Phys. Rev. **109**, 1396 (1958).

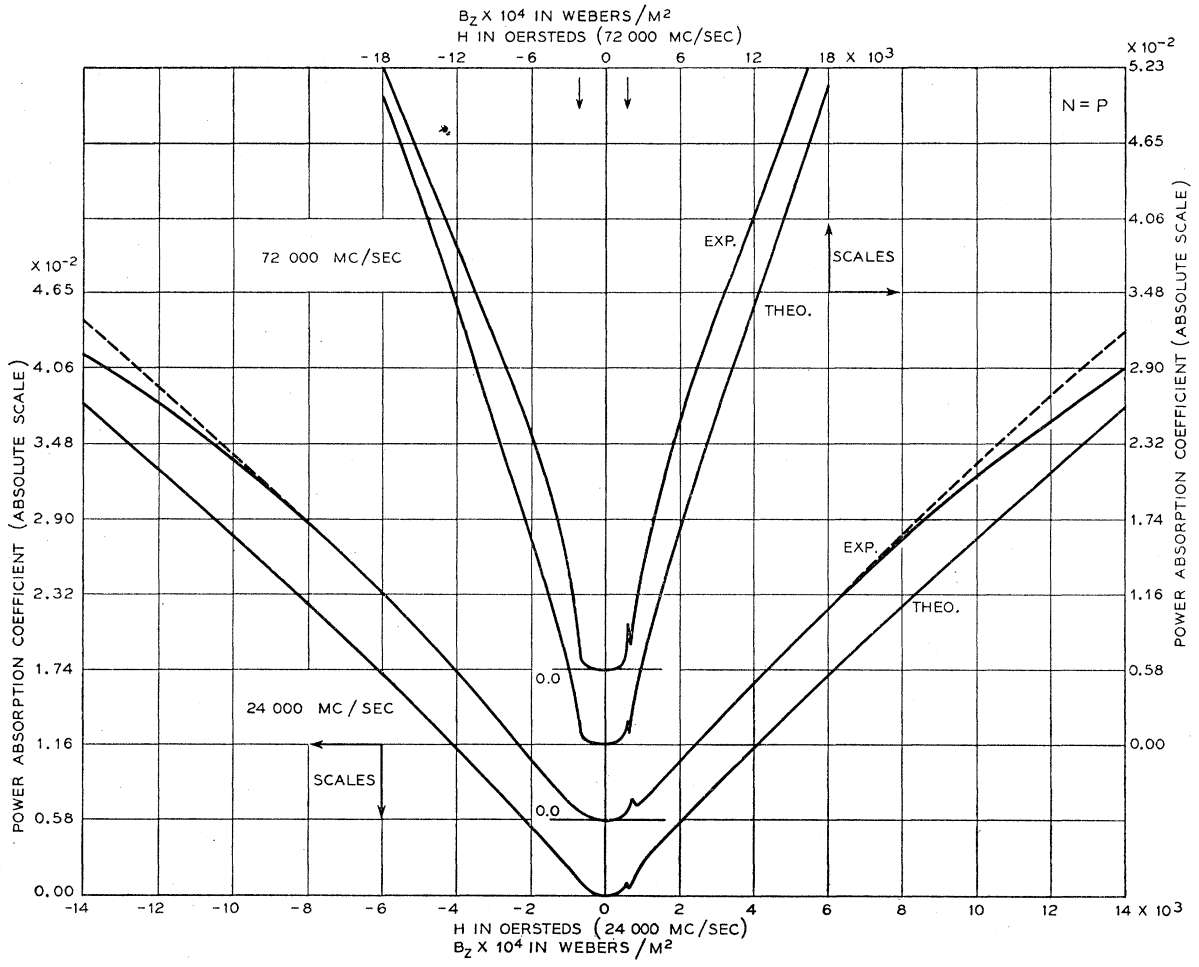

FIG. 4. Plots of power absorption coefficient *vs* magnetic field from both theory and experiment with magnetic field normal to sample surface and along a three-fold axis in pure bismuth. Curves for two frequencies are shown and the ordinate scales give absolute values. Zero absorptivity for the experimental curves is offset vertically from that for the theoretical curves, and its position is indicated on the vertical axis at zero field. The magnetic field scale used at 72 000 Mc/sec is compressed by a factor three with respect to that used at 24 000 Mc/sec so that the cyclotron field for a given set of carriers is on the same vertical line for all curves. Vertical arrows indicate these fields; there is one for electrons and one for holes. The curves show sharp changes at the electron cyclotron field on both sides of $B=0$ because of the anisotropy of the electron bands, but the holes only introduce a singularity at their cyclotron field on one side, since their band is isotropic about a three-fold axis. The relaxation times used in calculating the theoretical curve at 72 000 Mc/sec are such that for holes $\omega\tau=20$ and for electrons $\omega\tau=30$. At 24 000 Mc/sec the same values of $\omega\tau$ were used. The dashed line shows how the experimental curve at 24 000 Mc/sec would look in the absence of the saturation which occurs in the experiments at that frequency.

show the singularities so well resolved one from another. When B_z was in the plane of the sample, we continued to use radiation which was circularly polarized about a normal to this plane in taking the data. Data taken under these conditions with linear polarization will be reported later.

Experiments have been performed at various temperatures from 300°K to 1.06°K, but the results are insensitive to temperature below 4.2°K, and show a lack of resolution due to thermal scattering at high temperatures. As a result, only data taken at approximately 1.3°K is presented.

Figure 3 shows data obtained at both experimental frequencies on pure bismuth with magnetic field along a two-fold axis and normal to the surface of the sample. Figures 4 and 5 show data taken on pure bismuth samples in the same way but with the magnetic field along three-fold and bisectrix axes, respectively.

Figure 6 shows results obtained at 72 000 Mc/sec with magnetic field parallel to the surface of the sample in pure bismuth; each of the three curves gives the data obtained with the magnetic field parallel to one of the three principal axes. There is at present no satisfactory theoretical analysis for the data in Fig. 6, but the *positions* of the singularities can be interpreted in terms of suggestions by Anderson[28] and the theory of Azbel' and Kaner.[23] This was useful in improving the accuracy of the values of some of the cyclotron masses deduced

from data taken with the field normal to the sample surface.

Figures 7 through 14 show data for alloys of bismuth with tin and tellurium with B_z perpendicular to the sample surface and along two-fold and three-fold axes. For each sample data is shown at both experimental frequencies. The compositions of samples such that B_z is along a two-fold axis are not identical with those of samples such that B_z is along a three-fold axis, but a distribution of compositions is shown for both orientations. The ratio of the number of holes to the number of electrons is given for each alloy in the relevant figure caption. The ratio given is the one which gives the best fit between the theoretical curve and the experimental data.

Figure 8 shows data similar to those previously published by some of us.[31] The sample used in the previous experiments has now been found to have a pseudo-three-fold axis normal to its surface, rather than the trigonal axis in bismuth. The present results also show that it was not pure bismuth electrically. However the early data show clearly the presence of a majority carrier which is a hole of cyclotron mass about 0.3, and a minority which is an electron. The anisotropy effects

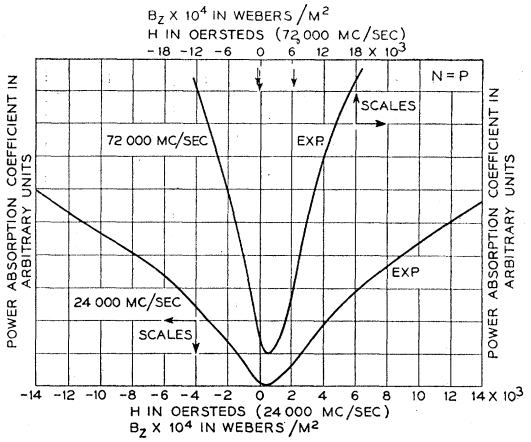

FIG. 5. Plot of power absorption coefficient *vs* magnetic field from experiment only with magnetic field normal to sample surface and along a bisectrix axis in pure bismuth. Curves for two frequencies are shown, but because no theoretical analysis is available for this case, the ordinates are in arbitrary units. The magnetic field scale used at 72 000 Mc/sec is compressed by a factor three with respect to that used at 24 000 Mc/sec so that the cyclotron field for a given set of carriers is on the same vertical line for both curves. Vertical arrows indicate these fields as determined from the theory and other data; there are two electrons and one hole. Although no quantitative theory of these data is available, it is quite clear by inspection of the broad variations on both sides of $B=0$ that the holes must have higher masses than the electrons.

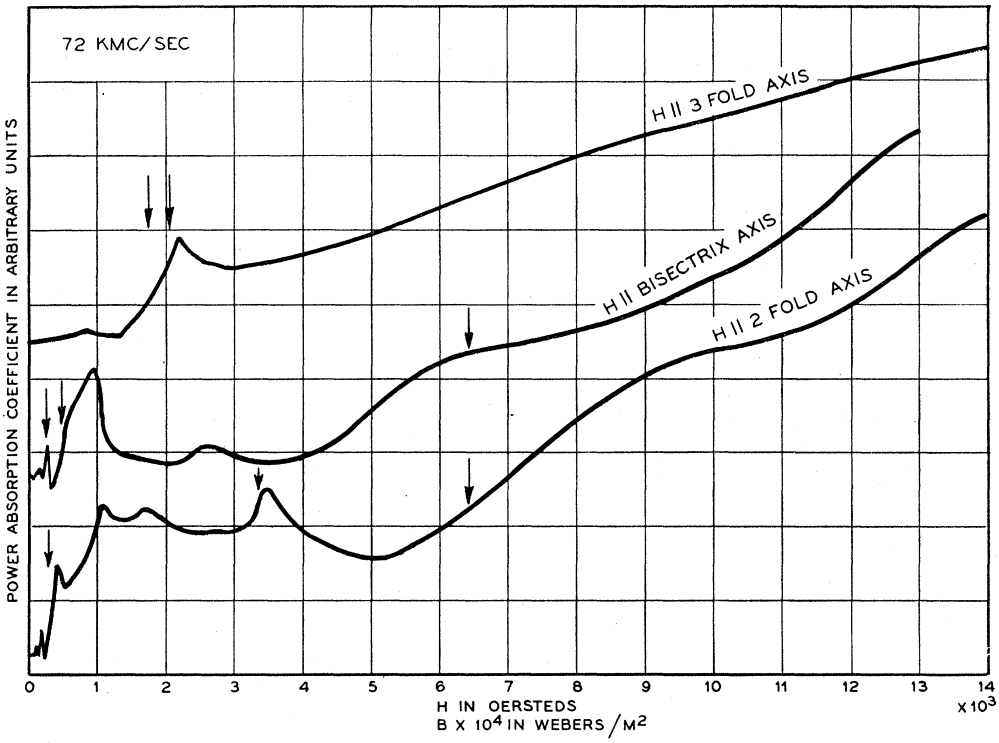

FIG. 6. Plot of power absorption coefficient *vs* magnetic field from experiment only with magnetic field in the plane of the sample in pure bismuth. The different curves give data taken with magnetic field along the different principal crystal directions. All these data were observed at 72 000 Mc/sec, and the ordinates are in arbitrary units. Vertical arrows indicate the cyclotron fields on each curve. These fields are the same as those indicated in the previous three figures for the corresponding crystallographic directions. Singularities are well resolved at the cyclotron fields corresponding to the lower mass carriers. The peak near 1000 oe in the data taken with magnetic field parallel to bisectrix and twofold axes is thought to arise from a dielectric anomaly. The radiation was circularly polarized about a normal to the sample surface when these data were obtained.

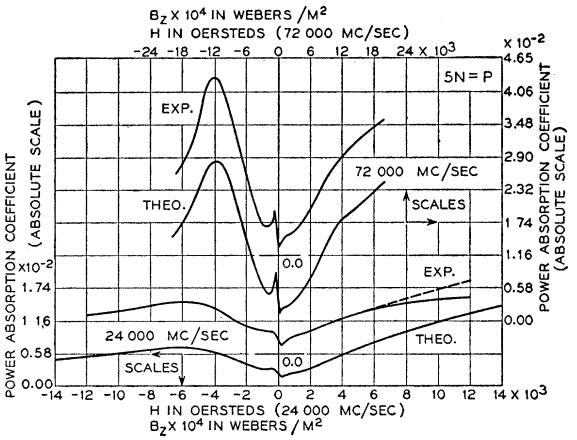

FIG. 7. Plots of power absorption coefficient *vs* magnetic field from both theory and experiment with magnetic field normal to sample surface and along a two-fold axis in an alloy of bismuth and tin. The amount of tin present is such that the number of holes is 5 times the number of electrons ($5N=P$). The relaxation times used in calculating the theoretical curve at 72 000 Mc/sec give for holes $\omega\tau=4$ and for electrons $\omega\tau=1.5$. At 24 000 Mc/sec the values are for holes $\omega\tau=1.5$ and for electrons $\omega\tau=0.5$. The magnetic field scales are adjusted so that the cyclotron field for a given set of carriers is on the same vertical line for all curves. As with pure bismuth in this orientation, shown in Fig. 3, the fit between theory and experiment could be improved still further if the theory allowed us to use separate relaxation times for high-mass and low-mass electrons. The dashed line shows how the experimental curve at 24 000 Mc/sec would look in the absence of the saturation which occurs in the experiments at that frequency.

make it impossible to estimate the electron cyclotron mass.[36]

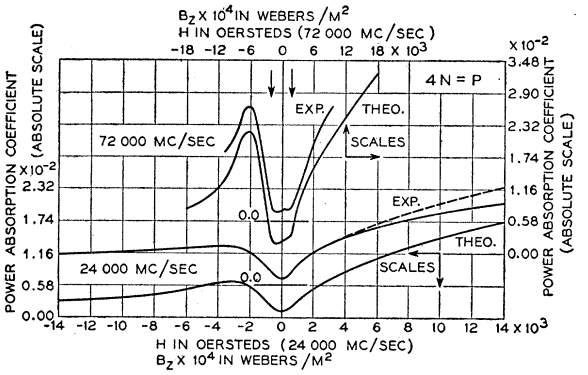

FIG. 8. Plots of power absorption coefficient *vs* magnetic field from both theory and experiment with magnetic field normal to sample surface and along a three-fold axis in an alloy of bismuth and tin. The amount of tin present is such that the number of holes is 4 times the number of electrons ($4N=P$). The relaxation times used in calculating the theoretical curve at 72 000 Mc/sec give for holes $\omega\tau=0.5$ and for electrons $\omega\tau=5$. At 24 000 Mc/sec the values are for holes $\omega\tau=0.25$ and for electrons $\omega\tau=1.5$. The magnetic field scales are adjusted so that the cyclotron field for a given set of carriers is on the same vertical line for all curves. The data taken at 72 000 Mc/sec did not extend beyond 10^4 oe for this sample. In this case the experimental curve at 24 000 Mc/sec is a composite of two taken in such a way as to reduce the saturation effects at this frequency. The dashed line shows how the data would look in the absence of this saturation.

[36] M. Tinkham, Phys. Rev. **101**, 902 (1956).

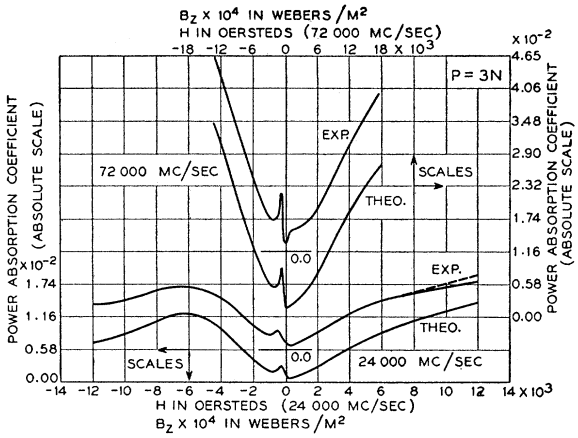

FIG. 9. Plots of power absorption coefficient *vs* magnetic field from both theory and experiment with magnetic field normal to sample surface and along a two-fold axis in an alloy of bismuth and tin. The amount of tin present is such that the number of holes is 3 times the number of electrons ($3N=P$). The relaxation times used in calculating the theoretical curve at 72 000 Mc/sec give for holes $\omega\tau=2.5$ and for electrons $\omega\tau=1.5$. At 24 000 Mc/sec the values are for holes $\omega\tau=2$ and for electrons $\omega\tau=1.3$. The magnetic field scales are adjusted so that the cyclotron field for a given set of carriers is on the same vertical line for all curves. The dashed line shows how the experimental curve at 24 000 Mc/sec would look in the absence of the saturation which occurs in the experiments at that frequency. The misfit between theory and experiment at low fields at 72 000 Mc/sec in this case is not understood.

IV. ANALYSIS

We now present a theory on the basis of which the data given in the previous section can be interpreted. The physically significant aspects of this theory are

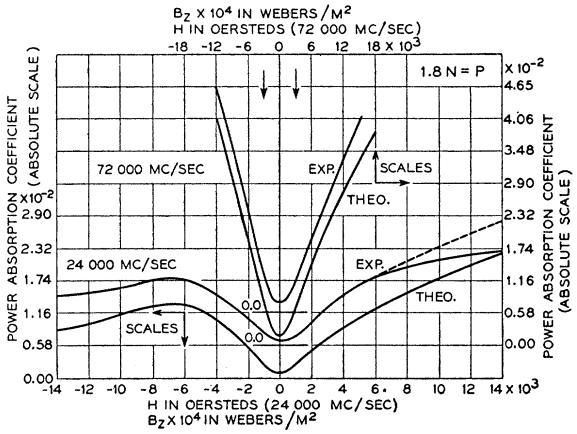

FIG. 10. Plots of power absorption coefficient *vs* magnetic field from both theory and experiment with magnetic field normal to sample surface and along a three-fold axis in an alloy of bismuth and tin. The amount of tin present is such that the number of holes is 1.8 times the number of electrons ($1.8\,N=P$). The relaxation times used in calculating the theoretical curve at 72 000 Mc/sec give for holes $\omega\tau=1.5$ and for electrons $\omega\tau=2$. At 24 000 Mc/sec the values are for holes $\omega\tau=0.5$ and for electrons $\omega\tau=1.5$. The magnetic field scales are adjusted so that the cyclotron field for a given set of carriers is on the same vertical line for all curves. The dashed line shows how the experimental curve at 24 000 Mc/sec would look in the absence of the saturation which occurs in the experiments at that frequency.

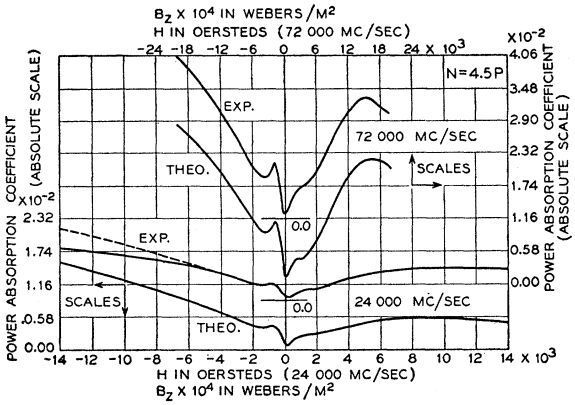

FIG. 11. Plots of power absorption coefficient *vs* magnetic field from both theory and experiment with magnetic field normal to sample surface and along a two-fold axis in an alloy of bismuth and tellurium. The amount of tellurium present is such that the number of electrons is 4.5 times the number of holes ($N=4.5\,P$). The relaxation times used in calculating the theoretical curve at 72 000 Mc/sec give for holes $\omega\tau=1.5$ and for electrons $\omega\tau=1.5$. At 24 000 Mc/sec the values are for holes $\omega\tau=0.5$ and for electrons $\omega\tau=1.5$. The magnetic field scales are adjusted so that the cyclotron field for a given set of carriers is on the same vertical line for all curves. The dashed line shows how the experimental curve at 24 000 Mc/sec would look in the absence of the saturation which occurs in the experiments at that frequency.

best understood by starting with a discussion of the cyclotron resonance phenomenon for a material which has a single group of isotropic charge carriers. For the same reason, the conductivity of charge carriers will be dealt with as a contribution to the complex dielectric

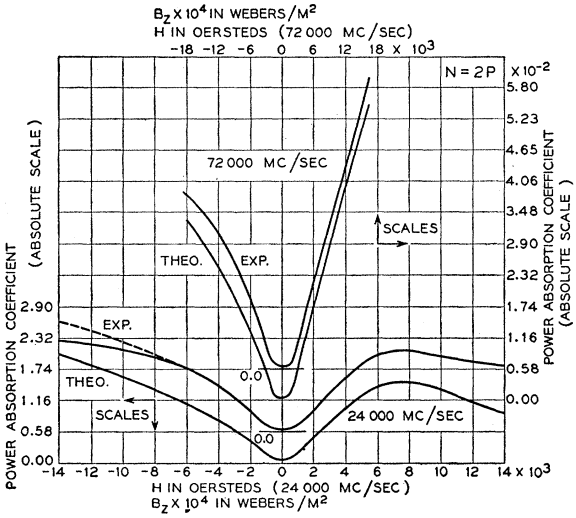

FIG. 12. Plots of power absorption coefficient *vs* magnetic field from both theory and experiment with magnetic field normal to sample surface and along a three-fold axis in an alloy of bismuth and tellurium. The amount of tellurium present is such that the number of electrons is 2 times the number of holes ($N=2P$). The relaxation times used in calculating the theoretical curve at 72 000 Mc/sec give for holes $\omega\tau=0.5$ and for electrons $\omega\tau=6$. At 24 000 Mc/sec the values are for holes $\omega\tau=1.0$ and for electrons $\omega\tau=1.5$. The magnetic field scales are adjusted so that the cyclotron field for a given set of carriers is on the same vertical line for all curves. The dashed line shows how the experimental curve at 24 000 Mc/sec would look in the absence of the saturation which occurs in the experiments at that frequency.

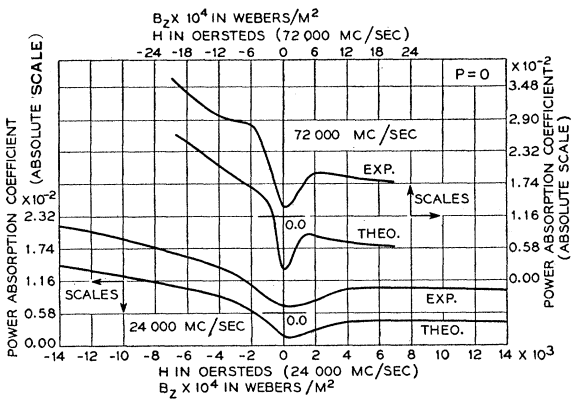

FIG. 13. Plots of power absorption coefficient *vs* magnetic field from both theory and experiment with magnetic field normal to sample surface and along a two-fold axis in an alloy of bismuth and tellurium. The amount of tellurium present is such that the number of holes is insignificant. The relaxation times used in calculating the theoretical curve at 72 000 Mc/sec give for holes $\omega\tau=1.0$ and for electrons $\omega\tau=0.8$. At 24 000 Mc/sec the values are for holes $\omega\tau=0.3$ and for electrons $\omega\tau=0.25$. The magnetic field scales are adjusted so that the cyclotron field for a given set of carriers is on the same vertical line for all curves. The effect was sufficiently small in this case so that no saturation is apparent in the 24 000 Mc/sec results. The fit between theory and experiment could be improved still further if the theory allowed us to use separate relaxation times for the high mass and the low mass electron. On the other hand the nature of the misfit also suggests that the electron effective masses in this alloy are somewhat higher than those in pure bismuth.

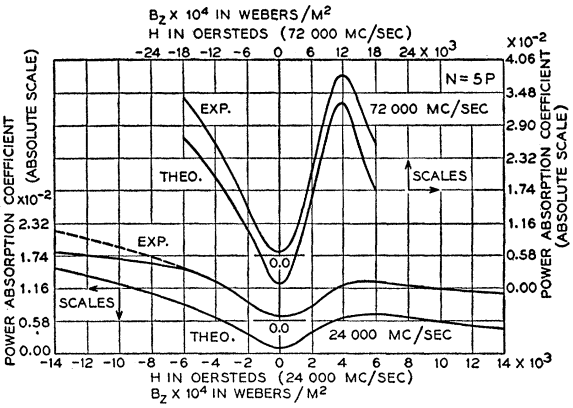

FIG. 14. Plots of power absorption coefficient *vs* magnetic field from both theory and experiment with magnetic field normal to sample surface and along a three-fold axis in an alloy of bismuth and tellurium. The amount of tellurium present is such that the number of electrons is 5 times the number of holes ($N=5P$). The relaxation times used in calculating the theoretical curve at 72 000 Mc/sec give for holes $\omega\tau=1$ and for electrons $\omega\tau=3$. At 24 000 Mc/sec the values are for holes $\omega\tau=0.25$ and for electrons $\omega\tau=1$. The magnetic field scales are adjusted so that the cyclotron field for a given set of carriers is on the same vertical line for all curves. The dashed line shows how the experimental curve at 24 000 Mc/sec would look in the absence of the saturation which occurs in the experiments at that frequency. The fit between experimental and theoretical curves is good except at low fields; the experimental curves stay flat to higher fields than do the theoretical ones. This indicates strongly that the electron effective masses in this alloy are larger than in pure bismuth.

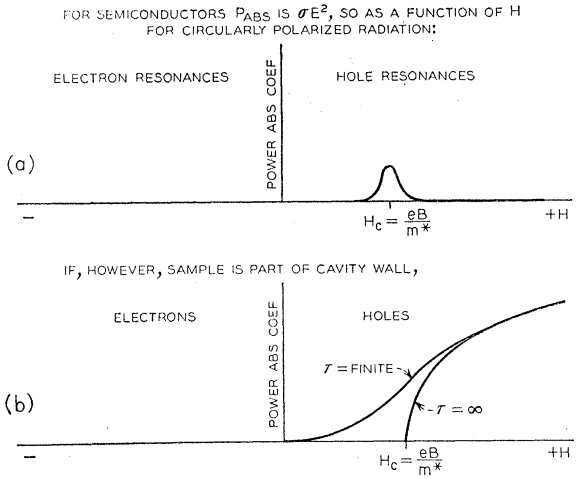

FIG. 15. (a) Schematic plot of power absorption coefficient *vs* magnetic field in cyclotron absorption experiment performed on a semiconductor with one charge carrier. (b) Schematic plot of power absorption coefficient *vs* magnetic field in a cyclotron absorption experiment on a metal with one group of isotropic charge carriers when the magnetic field is normal to sample surface.

constant ϵ of the material, which then has the form[29]:

$$\epsilon = \epsilon_l - j\sigma/\omega\epsilon_0, \tag{6}$$

in rationalized mks units, where ϵ_l is the contribution of the lattice exclusive of the charge carriers, ϵ_0 is the electric inductive capacity for free space and σ is a suitable solution of Eq. (1). *The dielectric constant of a medium is defined here as the ratio of its electric inductive capacity to that of free space.* Each term in Eq. (6) is in general a tensor. In the case of a circularly polarized wave propagated parallel to the steady magnetic field B_z in an isotropic medium, the dielectric constant for the propagation of the wave need not be expressed as a tensor, however. It is [19,26–28]:

$$\epsilon = \epsilon_l - \frac{jne^2\tau}{m\epsilon_0\omega[1+j(\omega-\omega_c)\tau]}. \tag{7}$$

Here n is the density of carriers, and the other quantities have been defined in connection with Eqs. (1), (2), and (6).

In the semiconductor experiment, the sample is placed within the cavity and the power absorption due to the resonance in the imaginary part of $\epsilon(\omega)$ is observed. The absorption as a function of B_z is plotted schematically in Fig. 15(a). As stated in Sec. I, to observe the resonance in metals, where the charge carrier density is high, the sample is made to form part of the cavity wall. With this arrangement the absorptivity of the specimen at normal incidence is measured. This is given in this simple case where $|\epsilon| \gg 1$ by:

$$A = 4\,\mathrm{Re}(1/\sqrt{\epsilon}), \tag{8}$$

where ϵ is defined by Eqs. (6) and (7). We see from Eqs. (7) and (8) that the signal depends mainly upon the behavior of the real part of $\epsilon(\omega)$ when $|(\omega-\omega_c)\tau| \gg 1$. This reflects the fact that under these conditions A is primarily determined by the discontinuity in electrical properties at the surface rather than by intrinsic absorption in the sample. Thus Eq. (7) shows that the real part of ϵ will be negative at fields such that the cyclotron frequency ω_c is below the experimental frequency ω, since the contribution of ϵ_l to the real part of ϵ is negligible at microwave frequencies. Equation (8) shows that the medium will be reflecting in this region. When ω_c is larger than ω, Eq. (7) shows that the real part of ϵ is positive, and in this region Eq. (8) shows that absorption occurs. The absorptivity as a function of magnetic field for this simple case is shown schematically[28] in Fig. 15(b) for two different collision times.

The present work is concerned with the extension of these ideas to more complicated cases. Qualitatively, it is easy to see the different behavior to be expected. In the first place, if constant energy contours normal to the steady applied field are not isotropic but ellipsoidal, the cyclotron resonance for a given carrier group is excited by both circular polarizations to some extent.[36] In this case some care is needed in deciding the sign of the charge of the carrier group responsible for a given feature of the absorptivity *vs* B_z curve. In fact, although it does not occur in bismuth, still lower symmetries in the constant energy contours give rise to resonance at harmonics of the fundamental cyclotron frequency.[37]

In the second place, the complexity of the results is increased if more than one group of charge carriers is present, even in the absence of anisotropy. There are two reasons for this. One is that there is a singularity at the cyclotron field for each of the charge carriers. A second is apparent from the topology of the dispersion curves which occur at each cyclotron field in the plot of the real part of ϵ *vs* B_z. Consider a case in which there are more than one charge carrier mass for the same sign of charge and circularly polarized incident radiation. There will in general always be a field somewhere away from the cyclotron fields and between each pair of them at which the contributions of the charge carriers to the real part of ϵ cancel to give zero for the net total value of the real part of ϵ (and near it, a value the same as that for free space). This cancellation is illustrated schematically for two charge carriers in Fig. 16. A similar cancellation can occur when the carriers consist of one electron and one hole when their numbers are unequal. A similar phenomenon which occurred because of a slightly different type of cancellation in contributions to Re ϵ has recently been named a "dielectric anomaly,"[35] and we shall use that term in this paper. Singularities of this type influence the shape of our

[37] Galt, Yager, and Dail, Phys. Rev. **103**, 1586 (1956); P. Nozières, Phys. Rev. **109**, 1510 (1958); B. Lax and H. J. Zeiger, Phys. Rev. **105**, 1466 (1957).

results considerably; they occur at values of B_z and ω at which it is presumably possible to excite plasma waves.[29,30]

The solution of the general electromagnetic problem presented here follows the standard method. First the propagation vector is derived in terms of the effective dielectric constant and then the boundary value problem at the metal surface is solved. The system considered is that of an electromagnetic wave normally incident upon the infinite surface of a metal which we suppose defines the xy plane of our coordinate system, the interior of the metal corresponding to the region $z>0$. The steady magnetic field B_z is parallel to $\pm z$. It will be assumed that the magnetoconductivity tensor has the form:

$$\sigma=\begin{bmatrix}\sigma_{xx} & \sigma_{xy} & 0\\ \sigma_{yx} & \sigma_{yy} & 0\\ 0 & 0 & \sigma_{zz}\end{bmatrix}, \tag{9}$$

or a permutation of this form. Explicit expressions for the $\sigma_{\mu\nu}$ will be given later. It is important to note that this assumption implies that the **B** field is along the z axis, and that an **E** field in the xy plane gives rise to a current which is restricted in direction to the xy plane. If this were not the case, depolarizing effects would again enter the problem. It is further assumed that the waves have constant phase planes in the medium (bismuth) which are normal to the z axis, so that derivatives with respect to x and y vanish. Maxwell's equations inside the medium become:

$$\begin{aligned}&\frac{\partial^2 E_x}{\partial z^2}-\mu_0\epsilon_0\epsilon_l\frac{\partial^2 E_x}{\partial t^2}-\frac{\partial J_x}{\partial t}=0,\\ &\frac{\partial^2 E_y}{\partial z^2}-\mu_0\epsilon_0\epsilon_l\frac{\partial^2 E_y}{dt^2}+\frac{\partial J_y}{dt}=0,\\ &E_z=0.\end{aligned} \tag{10}$$

The plane wave solutions have the form:

$$\begin{aligned}E_x&=E_{x0}\exp j(\omega t-kz),\\ E_y&=E_{y0}\exp j(\omega t-kz).\end{aligned} \tag{11}$$

From Eqs. (10) and (11), we find that the amplitudes E_{x0} and E_{y0} satisfy:

$$\begin{aligned}(\eta^2-\epsilon_{xx})E_{x0}-\epsilon_{xy}E_{y0}&=0,\\ -\epsilon_{yx}E_{x0}+(\eta^2-\epsilon_{yy})E_{y0}&=0,\end{aligned} \tag{12}$$

where $\eta=k/k_0$, and $k_0=\omega/c$ is the wave vector in free space. The $\epsilon_{\mu\nu}$ are components of the dielectric constant tensor as defined by Eqs. (6) and (9):

$$\epsilon_{\mu\nu}=\epsilon_l\delta_{\mu\nu}-j\sigma_{\mu\nu}/\omega\epsilon_0. \tag{13}$$

Equations (12) are consistent only if:

$$\eta=\pm\{\tfrac{1}{2}(\epsilon_{xx}+\epsilon_{yy})\pm[(\epsilon_{xx}-\epsilon_{yy})^2/4+\epsilon_{xy}\epsilon_{yx}]^{\frac{1}{2}}\}^{\frac{1}{2}}, \tag{14}$$

and Eq. (14) therefore defines the propagation constants

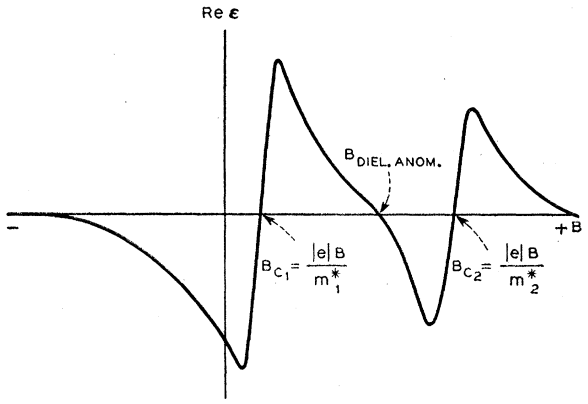

FIG. 16. Schematic plot of the contribution of two isotropic charge carriers of the same sign to the real part of the dielectric constant relevant to the propagation of a circularly polarized wave through an infinite medium. The real part of this dielectric constant is plotted *vs* magnetic field, and it will be noted that it passes through zero at a point between the two cyclotron fields. This point is labeled a dielectric anomaly.

which characterize the waves in the medium. The η's are in general complex, and the ones desired are those in the fourth quadrant, which characterize damped waves traveling toward positive z. Two of the four possible values of η always fulfill this condition. The waves which these propagation constants characterize are in general elliptically polarized, and they will be distinguished by a superscript $+$ or $-$, thus: η^+ and η^-. The components of these waves are related thus:

$$E_{y0}{}^{\pm}=\alpha^{\pm}E_{x0}{}^{\pm}, \tag{15}$$

where from Eqs. (12):

$$\alpha^{\pm}=(\eta^{\pm 2}-\epsilon_{xx})/\epsilon_{xy}=\epsilon_{yx}/(\eta^{\pm 2}-\epsilon_{yy}). \tag{16}$$

It can also be shown from Eqs. (14) and (16):

$$\alpha^+\alpha^-=-\epsilon_{yx}/\epsilon_{xy}. \tag{17}$$

The component amplitudes of the reflected wave E^r are now obtained in terms of the component amplitudes of the incident wave E^i by requiring the tangential field components to be continuous at the boundary. Given an incident wave normal to the surface, there results, after some algebraic manipulation:

$$\begin{aligned}E_{x0}{}^r&=\{(\alpha^+Z^--\alpha^-Z^+)E_{x0}{}^i+(Z^+-Z^-)E_{y0}{}^i\}\\ &\quad\times\{1/(\alpha^+-\alpha^-)\},\\ E_{y0}{}^r&=\{-\alpha^+\alpha^-(Z^+-Z^-)E_{x0}{}^i+(\alpha^+Z^+-\alpha^-Z^-)E_{y0}{}^i\}\\ &\quad\times\{1/(\alpha^+-\alpha^-)\}.\end{aligned} \tag{18}$$

Here:

$$Z^{\pm}=(1-\eta^{\pm})/(1+\eta^{\pm}). \tag{19}$$

The power reflection coefficient is given in general by:

$$R=(|E_{x0}{}^r|^2+|E_{y0}{}^r|^2)/(|E_{x0}{}^i|^2+|E_{y0}{}^i|^2), \tag{20}$$

and in the case of a circularly polarized incident wave

where $E_{y0}{}^{i}=jE_{x0}{}^{i}$ by:

$$R=\tfrac{1}{2}[|E_{x0}{}^{r}|^2/|E_{x0}{}^{i}|^2+|E_{y0}{}^{r}|^2/|E_{x0}{}^{i}|^2]. \quad (21)$$

The absorptivity, A, is given by:

$$A=1-R. \quad (22)$$

The analysis contained in Eqs. (10) through (22) has been used to obtain theoretical plots of absorptivity *vs* B_z which were compared with the experimental curves to determine the effective mass parameters in bismuth. Such calculations must be based upon some model of the band structure. Magnetic and transport properties indicate that there are only a small number of free carriers. According to Jones,[38] this is due to the overlap of a few electrons across the zone boundaries in momentum space, an equal number of holes being left in the lower zone. Shoenberg[39] has interpreted his measurements of the de Haas-van Alphen effect in terms of an electron band consisting of a family of six ellipsoids. A typical one, referred to an origin at its center, is of the form:

$$E=(1/2m_0)(\alpha_1 p_1{}^2+\alpha_2 p_2{}^2+2\alpha_4 p_2 p_3+\alpha_3 p_3{}^2), \quad (23)$$

where p_1, p_2, p_3 are momentum components parallel to the binary, bisectrix and trigonal axes, respectively; m_0 is the free electron mass and the α's are components of the reciprocal of the effective mass tensor. For the ellipsoid given by Eq. (23) the latter has the form:

$$m=\begin{bmatrix} m_1 & 0 & 0 \\ 0 & m_2 & m_4 \\ 0 & m_4 & m_3 \end{bmatrix}, \quad (24)$$

where m_1, m_2, m_3, m_4 are effective masses in units of m_0. If the ellipsoid is located on a mirror plane, two further ellipsoids may be generated by rotation through $\pm 120°$ and the remaining three obtained by inversion through the origin (point group D_{3d} or $R_{3m}{}^{-}$). The de Haas-van Alphen effect did not exhibit any oscillations which could be attributed to the hole band. Consequently the model for the holes proposed by Abeles and Meiboom[33] has been adopted in the present work to explain the galvanomagnetic properties of bismuth. This is a single ellipsoid of revolution about the trigonal axis:

$$E=E_b-(1/2m_0)(p_1{}^2/M_1+p_2{}^2/M_1+p_3{}^2/M_3), \quad (25)$$

where E_b is the band overlap energy and M_1, M_3 are effective hole masses in units of m_0. The absence of an M_4 makes it unnecessary to introduce α's in this case.

Assuming isotropic collision times for electrons and holes, the conductivity tensor for this band model has previously been calculated by Lax, Button, Zeiger, and Roth.[27] For ease of reference, their results are reproduced in Appendix A together with expressions for the various cyclotron masses which occur for different orientations of the steady magnetic field relative to the crystal axes. Reference to Appendix A shows that with the magnetic field along either the trigonal or binary axes, the conductivity tensor is of the form given by Eq. (9) and attention has therefore been focussed in the present work upon these two orientations in making detailed calculations. Calculations were done with IBM 650 and 704 computing machines. Cyclotron masses were read directly from the data, and component masses computed from them using the formulae in Appendix A. Infrared data[35] has shown that the dielectric constant of the lattice exclusive of the charge carriers is 9, and this is negligible in the present work. The number of electrons in pure bismuth, which is equal to the number of holes, is assumed in these calculations to be 4.2×10^{17}/cm^3. This value is obtained from previous work on the de Haas-van Alphen observations[39] and the resistivity of bismuth alloys.[34] Further confirmation of this number has been obtained from chemical analysis of the sample for which data are shown in Fig. 8. The number of charge carriers is obtained from (1) the amount of tin in the sample, which is 1 part in 10^5, (2) the fact that $P=4N$ in this sample; this is shown by the fit between theory and experiment independently of what is assumed for the total number of charge carriers, (3) the assumption that each tin atom removes one conduction electron from the Fermi sea of the bismuth. In the alloy calculations, where the number of holes and the number of electrons is unequal it was assumed that the sum of the number of electrons and the number of holes remains 8.4×10^{17}/cm^3. The absorptivity is proportional to the reciprocal of the square root of this number [see Eqs. (7) and (8)], so the theoretical results are not sharply dependent upon it.

Care must be taken in interpreting the low field resonance lines in terms of cyclotron masses. In fact, the absorption peaks bear no direct relation to the cyclotron fields but are the location of dielectric anomalies between two resonances as indicated by Fig. 16. It is for this reason we emphasized this point at the beginning of this section. Cyclotron resonance fields are the points at which the absorptivity extrapolates to zero as indicated by Fig. 15(b). This is true even for the lower mass carriers whose effect is limited to a relatively small range of fields by the dielectric anomaly effects and by the presence of other cyclotron resonances. It seems empirically to be true also when B_z is in the plane of the sample, at least in first approximation.

It will be noted from Eqs. (18) that polarization conversion occurs at the surface. An incident wave polarized along the x direction say, will in general give rise to an elliptically polarized reflected wave. Similarly, if the incident wave is circularly polarized, two counter-rotating circularly polarized waves will be reflected in general. This point has been mentioned previously in Sec. II and means that with the experimental arrangement used in the present work some of the power re-

[38] H. Jones, Proc. Roy. Soc. (London) **A147**, 396 (1934); **A155**, 653 (1936).
[39] D. Shoenberg, Proc. Roy. Soc. (London) **A170**, 341 (1939).

radiated from the cavity will travel toward the detector. Variations in such a signal would constitute an error since the variation in the signal at the detector is interpreted to be proportional to the variation in the absorptivity of the sample. However, if we assume that the theory given above is correct, we can calculate from E_{x0}^r and E_{y0}^r the fractional part of the reflected power which is of the wrong circularity. Changes in this quantity as the magnetic field varies are equal to the magnitude of the error in the apparent *reflectivity* from this source. This calculation has been made for all the pure bismuth curves and for representative alloy cases. In the alloy cases, errors in the absorptivity are fractionally small. In pure bismuth there is no error of this kind at all when B_z is along a three-fold axis. When B_z is along a two-fold axis, the error is negligible for the most part, but at 72 000 Mc/sec it is significant at certain fields, and the dotted line in Fig. 3 shows how the data are changed if they are corrected by means of this calculation. A noticeable improvement in the fit between theory and experiment is produced by the correction in this case.

V. DISCUSSION

The results of the above theoretical analysis give considerable insight into the meaning of various features of the absorptivity curves. Consider Fig. 3, which shows data taken with B_z perpendicular to the plane of the sample and along a two-fold axis in pure bismuth. For the sake of brevity, and because it contains the best resolved data, only the 72 000 Mc/sec curve will be discussed in detail. The cyclotron fields which were finally decided upon are indicated by arrows at the top of the figure. At high fields on both sides of $B=0$ broad variations in absorptivity occur which are caused primarily by the highest mass carrier, a hole in this case. These broad variations extrapolate to zero absorptivity at about 6000 oe, corresponding approximately to the cyclotron mass of 0.25 indicated by one of the arrows, and one appears on each side of $B=0$ because of the ellipticity of cross sections of the hole band normal to a two-fold axis. At fields just below 6000 oe on both sides of $B=0$ there is a region where the absorptivity is primarily due to the high mass electron. This charge carrier affects the curve on both sides of $B=0$ because of the ellipticity of the cross section of the electron bands. It has a rather low $\omega\tau$ (probably about 1) and the curve therefore does not extrapolate very clearly to zero at the cyclotron field of 3350 oe, corresponding to the mass of 0.13 indicated by another of the arrows. For negative fields, the next feature of the curve as we go to smaller fields is a sharp peak in absorptivity. This peak is the result of a dielectric anomaly caused by the cancellation of the contributions of two groups of electrons to the real part of the relevant dielectric constant. One group of electrons is the one just discussed with cyclotron mass 0.13. The other has a mass of 0.0105, a cyclotron resonance field of 270 oe as indicated by the third arrow, and an $\omega\tau$ of about 10. On the positive field side the ellipticity of the bands causes a small peak from this carrier to appear, but the effect is much smaller and there is no dielectric anomaly apparent. Because the $\omega\tau$'s for the two groups of electrons are different, the theory, which only includes one value of $\omega\tau$ for all electrons, does not fit perfectly at fields below 4500 oe. The curve plotted in Fig. 3 assumes $\omega\tau=3$ for the electrons, and this is approximately the geometrical mean of the correct values for the two groups.

The curves shown in Fig. 4 are somewhat simpler than those in Fig. 3 because only one electron and one hole are involved. As before, the cyclotron fields are indicated by arrows at the top of the figure. They show data taken with B_z parallel to a three-fold axis and normal to the surface of the sample, and here again only the 72 000 Mc/sec data will be discussed explicitly. The broad variations in absorptivity at high fields on both sides of $B=0$ extrapolate in to zero at approximately 2000 oe, corresponding to the cyclotron mass of 0.08 indicated by one of the vertical arrows. The shape of these curves is affected by the presence of the holes, but the only feature explicitly identifiable with the holes is a small peak whose low-field side extrapolates to zero somewhat below 2000 oe, corresponding to the cyclotron mass of 0.068 which is obtained by fitting the curve with the quantitative theory. These data are rather sensitive in detail to the orientation of the magnetic field; they show more structure at low fields if B_z is a few degrees off the three-fold axis.

In Fig. 5 are shown data taken with B_z along a bisectrix axis and normal to the sample surface. The broad variations in absorptivity do not extrapolate to zero very satisfactorily in this case and no quantitative mass values can be read from the data, although it is clear that the electron masses are smaller than the hole masses. The interesting thing about Fig. 5 is that the data do not indicate the presence of two electrons in spite of the fact that the model of the electron band structure calls for two, as indicated by the arrows at the top of the figure. Further discussion of this point will be given below.

We do not have a quantitative theory for the data shown in Fig. 6, taken with B parallel to the sample plane on pure bismuth. However, the data do indicate the presence of singularities at the cyclotron fields as suggested by Anderson[28]; vertical arrows show these points. Furthermore, signals are apparent in some cases at fields corresponding to harmonics of the cyclotron frequency. These harmonic effects are apparent at 1700 oe and below 200 oe in the data taken with the magnetic field parallel to a two-fold axis. Frequencies twice the fundamental cyclotron resonance frequency are involved here and these should not arise from band asymmetry effects in this orientation.[37] This point will be discussed further below. The peak near 1000 oe in the data taken with the magnetic field parallel to two-

fold and bisectrix axes is thought to arise from a dielectric anomaly.

The data on alloys in Figs. 7 through 14 are important because they show how the absorptivity varies as we pass from samples with a hole majority through pure bismuth where the number of electrons and holes is equal, to samples with an electron majority. The $\omega\tau$'s are reduced in these materials, presumably by impurity scattering, and the cyclotron masses are therefore best read from data on pure bismuth. The fit between theory and experiment in the alloys, however, is such as to indicate that there is very little change in effective mass values from those for pure bismuth except in two cases. (See Figs. 13 and 14.)

The inherent shape of the absorption curve in the presence of a finite relaxation time even for a single isotropic group of carriers [Fig. 15(b)] is such that it was not always easy to read off cyclotron resonance fields accurately from the experimental data when the magnetic field was normal to the surface of the sample. To obtain more accurate values for some of the cyclotron resonance fields, the data obtained with the magnetic field parallel to the plane of the sample have also been used to some extent. While the detailed theory for this case has not been worked out, it has been shown[28] that resonances of certain groups of carriers should be observed, and indeed this is borne out by the data (see Fig. 6). The final check on this procedure is, of course, that the parameters so obtained should then give close agreement in comparisons of theory with experiment for B_z normal to the surface in the specified orientations.

The final values of the cyclotron masses read from the data are, for the electrons:

$B\|$ three-fold axis (axis 3):

$$m^*=0.080. \tag{26a}$$

$B\|$ two-fold axis (axis 1):

$$m_a^*=0.13,$$
$$m_b^*=0.0105. \tag{26b}$$

$B\|$ bisectrix axis (axis 2):

$$m_a^*=0.0091,$$
$$m_b^*=0.0180. \tag{26c}$$

And for the holes:

$B\|$ three-fold axis (axis 3):

$$M^*=0.068. \tag{27a}$$

$B\|$ two-fold axis (axis 1):

$$M^*=0.25. \tag{27b}$$

$B\|$ bisectrix axis (axis 2):

$$M^*=0.25. \tag{27c}$$

It is felt that all these numbers are valid to within 10%. Note that these are not the component masses used in the conductivity formulas, but functions of them which determine cyclotron resonance frequencies.

It should be emphasized that the data not only determine the masses in Eqs. (26) and (27) but also show that they are the *only* cyclotron masses in bismuth associated with a significant number of charge carriers and with masses less than about 2. Thus, for example, only one cyclotron resonance mass for the holes is observed for each crystallographic orientation of B_z. This strongly supports the one ellipsoid model for the holes suggested by Abeles and Meiboom.[33] Furthermore, the data with B_z along a bisectrix axis show that, as suggested by Shoenberg,[39] the ellipsoids in the electron band are tilted, i.e., $m_4\neq 0$. To see this, note that if B_z is parallel to the sample plane (see Fig. 6) two cyclotron masses are resolved which fit the electron band model, but if B_z is perpendicular to the sample plane and still along the bisectrix (see Fig. 5) only the broad variation in absorptivity associated with fields above the cyclotron resonance of the highest mass carrier is observed. A broad variation in absorptivity associated with the holes is observed in each case. The absence of any singularity associated with a second electron when B_z is perpendicular to the sample plane is presumably associated with depolarizing effects which arise because in this orientation if $m_4\neq 0$, the conductivity tensor does not have zeros as does the one given in Eq. (9). Depolarizing effects result because under these circumstances a field $\mathbf{E}$ in the sample plane leads to a current with a component normal to the plane. The parameters which give a best fit to the data give added evidence that $m_4\neq 0$.

No harmonics of the cyclotron resonance of the sort which arise from the symmetry of the band structure are observed in bismuth.[37] This confirms the ellipsoidal symmetry of the bands, as assumed by the model. The second harmonic effects observed with the magnetic field in the plane of the sample (see Fig. 6) are such that the band symmetry cannot generate them. They are observed in the sample-field geometry postulated by Azbel' and Kaner,[23] and it is therefore felt that they indicate that the effects described by Azbel' and Kaner are incipient.

No evidence was found for a distribution of effective masses rather than a discrete set.[37] The frequency dependence of the line broadening behaved approximately as expected from relaxation time effects.

The effects of anisotropy in causing a response from the same group of charge carriers for both positive and negative values of B_z is apparent at many points in the data. In particular in Fig. 4 the absorptivity extrapolates to the electron cyclotron field for both signs of B_z. There is a small deviation for positive B_z at low absorptivities because of the resonance of the holes. Only the electrons are anisotropic about the magnetic field direction in this case.

The cyclotron masses for holes determine the component masses for the hole ellipsoid uniquely. These component masses are defined by Eq. (25). The values

obtained from the cyclotron masses are:

$$M_1=0.068, \quad M_3=0.92. \tag{28}$$

The component masses for the ellipsoids associated with the electron band are defined in Eqs. (23) and (24). From the cyclotron masses for the electrons, given in Eqs. (27), it is possible to determine the ratios of m_2, m_3, and m_4 to m_1, but not to determine m_1 itself accurately. The position of the absorption peak in the theoretical curves for the case B_z parallel to a two-fold axis is affected by changes in m_1, but not in a very sensitive way. Consequently, following a suggestion of W. S. Boyle, m_1 has been determined partly by means of information obtained from infrared observations. Dielectric anomalies have been observed in the infrared in bismuth at zero magnetic field[35] which correspond to the cancellation of the contributions of the charge carriers with that of the ionic lattice. The observations were made with plane polarized waves propagated along a two-fold axis, and the anomaly occurred at quite different frequencies for polarization parallel and perpendicular to a three-fold axis. It is possible to obtain an expression for this ratio from our formulae for η and the components of σ by assuming that at these points the relevant $\eta=0$. This expression depends on all the masses, and since we know everything but m_1, it can be used to calculate m_1. In this way, we find the following values for the component electron masses:

$$m_1=0.0088, \quad m_2=1.80, \quad m_3=0.023, \quad m_4=\pm 0.16. \tag{29}$$

The above electron mass components agree in order of magnitude with those obtained by Shoenberg, namely:

$$m_1=0.0024, \quad m_2=2.5, \quad m_3=0.05, \quad m_4=+0.25. \tag{30}$$

There is, however, substantial quantitative disagreement between the two sets. A possible source of error in de Haas-van Alphen effect measurements associated with the absolute amplitude of the oscillations has recently been pointed out by Aubrey and Chambers.[25] In interpreting their results from experiments using the Azbel'-Kaner[23] version of cyclotron resonance they found that the masses given by Shoenberg did not accurately locate the positions of their observed resonances. They suggested that Shoenberg's values of the mass ratios are correct, but that the absolute determination of one mass, which entailed measurement of absolute amplitude, was inaccurate. Using their values for the cyclotron masses with B_z along a binary axis, 0.11 and 0.0097 (which incidentally are in good agreement with our values of 0.13 and 0.0105) they obtain mass components:

$$m_1=0.006, \quad m_2=1.0, \quad m_3=0.02, \quad m_4=0.1, \tag{31}$$

which are in better agreement with the set of masses deduced from the present work.

Turning to the hole band, the masses observed in this work are all far smaller than the value of 1.5 m_0 suggested by Heine[40] to explain the effect of alloying in bismuth. It became evident in the course of making the present calculations that hole masses necessary to give this density of states mass were far too large to fit the data. The axial ratio for the hole ellipsoid M_1: $M_3=1:14.7$ may be compared with the ratio M_1: $M_3=1:3.7$ obtained by Abeles and Meiboom.[33] Agreement is only fair; this may be a consequence of the different electron band model for the electrons used in the analysis of the data.

[40] V. Heine, Proc. Phys. Soc. (London) **A69**, 513 (1956).

VI. ACKNOWLEDGMENTS

The authors wish to express their thanks to H. Dail, Jr., for technical assistance with the microwave work, to C. E. Miller for growing the bismuth crystals, to J. H. Wernick and K. E. Benson for providing zone refined pure bismuth, to S. P. Morgan for enlightening guidance on the theoretical work, to F. Barbieri for designing and building an acid cutting saw, to E. A. Wood for advice on crystal orientation problems, to K. H. Storks and C. L. Luke for chemical analysis of one of our specimens, to W. S. Boyle, D. Kleinman, and R. C. Fletcher for instructive conversations. We also wish to thank W. S. Boyle for suggestions on determining m_1 and W. S. Boyle, L. C. Hebel, Jr., W. Kohn, and P. A. Wolff for critical reading of the manuscript.

APPENDIX A

Label the two-fold, bisectrix, and three-fold axes as axis 1, axis 2 and axis 3, respectively; they form a cartesian set. Then the contribution of the electrons to the components of the conductivity tensor are:

B along three-fold axis (axis 3)

$$\begin{aligned}&\sigma_{11}/\sigma_0=\sigma_{22}/\sigma_0=(1/2\Delta)[(m_1+m_2)m_3-m_4^2],\\&\sigma_{12}/\sigma_0=-\sigma_{21}/\sigma_0=bm_3/\Delta, \quad \sigma_{33}/\sigma_0=(1/\Delta)\\&\qquad\qquad\times(m_1m_2+b^2),\\&\Delta_a=\Delta_b=\Delta_c=\Delta=m_1m_2m_3-m_1m_4^2+m_3b^2.\end{aligned} \tag{A1}$$

B along two-fold axis (axis 1)

$$\begin{aligned}&\frac{\sigma_{11}}{\sigma_0}=\frac{1}{3m_1}+\left(\frac{2}{3\Delta_c}\right)\left[\frac{(3m_1+m_2)m_3-m_4^2}{4}+b^2\right],\\&\frac{\sigma_{22}}{\sigma_0}=\frac{m_1m_3}{3\Delta_a}+\left(\frac{2}{3\Delta_c}\right)\left[\frac{(m_1+3m_2)m_3-3m_4^2}{4}\right],\\&\frac{\sigma_{33}}{\sigma_0}=\frac{m_1m_2}{3\Delta_a}+\frac{2m_1m_2}{3\Delta_c},\\&\frac{\sigma_{23}}{\sigma_0}=\frac{m_1(b-m_4)}{3\Delta_a}+\left(\frac{2}{3\Delta_c}\right)\left[\frac{(m_1+3m_2)}{4}b+\frac{m_1m_4}{2}\right],\\&\frac{\sigma_{32}}{\sigma_0}=-\frac{m_1(b+m_4)}{3\Delta_a}+\left(\frac{2}{3\Delta_c}\right)\left[\frac{m_1m_4}{2}-\frac{(m_1+3m_2)}{4}b\right],\\&\Delta_a=m_1(m_2m_3-m_4^2+b^2),\\&\Delta_b=\Delta_c=m_1m_2m_3-m_1m_4^2+\tfrac{1}{4}b^2(m_1+3m_2).\end{aligned} \tag{A2}$$

B along bisectrix axis (axis 2)

$$\frac{\sigma_{11}}{\sigma_0}=\frac{1}{3\Delta_a}(m_2m_3-m_4^2)+\left(\frac{2}{3\Delta_c}\right)\left[\frac{(3m_1+m_2)m_3-m_4^2}{4}\right],$$

$$\frac{\sigma_{22}}{\sigma_0}=\frac{1}{3\Delta_a}(m_1m_3+b^2)+\left(\frac{2}{3\Delta_c}\right)\left[\frac{(m_1+3m_2)m_3-3m_4^2}{4}+b^2\right],$$

$$\frac{\sigma_{33}}{\sigma_0}=\frac{m_1m_2}{3\Delta_a}+\frac{2m_1m_2}{3\Delta_c}, \tag{A3}$$

$$\frac{\sigma_{13}}{\sigma_0}=-\frac{\sigma_{31}}{\sigma_0}=-\frac{bm_2}{3\Delta_a}+\frac{2b}{3\Delta_c}\left(\frac{3m_1+m_2}{4}\right),$$

$$\sigma_{12}/\sigma_0=-\sigma_{21}/\sigma_0=-bm_4/\Delta_c,$$

$$\frac{\sigma_{23}}{\sigma_0}=\frac{\sigma_{32}}{\sigma_0}=\frac{m_1m_4}{3\Delta_a}+\frac{m_1m_4}{3\Delta_c},$$

$$\Delta_a=m_1m_2m_3-m_1m_4^2+m_2b^2,$$

$$\Delta_b=\Delta_c=m_1m_2m_3-m_1m_4^2+\tfrac{1}{4}(3m_1+m_2)b^2,$$

where

$$b=eB/[(1/\tau+j\omega)m_0] \quad \text{and} \quad \sigma_0=ne^2/[m_0(1/\tau+j\omega)],$$

n is the electron density, m_0 the mass of the free electron, $1/\tau$ the collision frequency, e the electron charge, and ω the angular frequency of the rf field.

To obtain the contribution of the holes to the corresponding tensor components, we simply let $m_4=0$, take only the terms involving Δ_a with the factor of $\frac{1}{3}$ omitted, and change the sign of b.

The expressions for the cyclotron masses are as follows:

$B\|$ axis 3,

$$m^*=m_0[(m_2m_3-m_4^2)m_1/m_3]^{\frac{1}{2}}; \tag{A4}$$

$B\|$ axis 1,

$$m_a^*=m_0(m_2m_3-m_4^2)^{\frac{1}{2}},$$

$$m_b^*=m_c^*=2m_0\left[\frac{m_1(m_2m_3-m_4^2)}{m_1+3m_2}\right]^{\frac{1}{2}}; \tag{A5}$$

$B\|$ axis 2,

$$m_a^*=m_0[(m_2m_3-m_4^2)m_1/m_2]^{\frac{1}{2}},$$

$$m_b^*=m_c^*=2m_0\left[\frac{m_1(m_2m_3-m_4^2)}{3m_1+m_2}\right]^{\frac{1}{2}}. \tag{A6}$$

The cyclotron masses for holes are:

$B\|$ axis 3:

$$m^*=(m_1m_2)^{\frac{1}{2}}=m_1; \tag{A7}$$

$B\|$ axis 1:

$$m^*=(m_2m_3)^{\frac{1}{2}}=(m_1m_3)^{\frac{1}{2}}; \tag{A8}$$

$B\|$ axis 2:

$$m^*=(m_1m_3)^{\frac{1}{2}}=(m_2m_3)^{\frac{1}{2}}. \tag{A9}$$

APPENDIX B

In the analysis we have used in interpreting the experiments we have neglected the diffusion of the charge carriers through the skin depth in calculating the current. When this approximation is not justified, the conditions are said to be anomalous, and the validity of our calculation is in question. We may estimate the range of magnetic field for which anomalous skin effect conditions prevail by generalizing an elementary argument given by Reuter and Sondheimer [see Eqs. (5) through (9) in reference 20] and noting the result in reference 22. For a single group of carriers of isotropic effective mass, one finds that conditions are anomalous if:

$$\frac{v_z\tau}{\{1+(\omega\pm\omega_c)^2\tau^2\}^{\frac{1}{2}}}\gg\frac{1}{|k|}, \tag{B1}$$

where v_z is the magnitude of the velocity normal to the sample surface, and $|k|$ the absolute magnitude of the complex propagation vector inside the sample. The sign in the $(\omega\pm\omega_c)$ term is determined by the circularity of the radiation used. Equation (B1) shows that, at resonance, conditions will be anomalous if $v_z\tau\gg\delta_0$, where δ_0 is the skin depth at zero magnetic field and at frequencies much smaller than the collision frequency, τ^{-1}. If $\omega\tau$ is large, however, it is clear that as the magnetic field changes and ω becomes different from ω_c, classical conditions prevail in certain field ranges even if $v_z\tau$ is greater than δ_0. Under these circumstances the experimental frequency is higher than those in the anomalous region.

In the experiments discussed here, more than one charge carrier is always present, and they are in general anisotropic, but near resonance for each charge carrier the bulk of the conduction is due to that carrier. Consequently, Eq. (B1) has been applied to several of the cases presented in the figures by comparing the calculated values of $|k|^{-1}$ with the left side of the equation computed near each resonance point for both circular polarizations using for v_z the component of the velocity normal to the sample surface of the charge carrier which resonates at that point. The propagation vectors were obtained from Eq. (14) and the definition of η; v_z was obtained from the relation $v_z=(2\epsilon_f/m_z)^{\frac{1}{2}}$, where ϵ_f is the Fermi energy, and m_z is the effective mass for motions *normal* to the sample surface. The

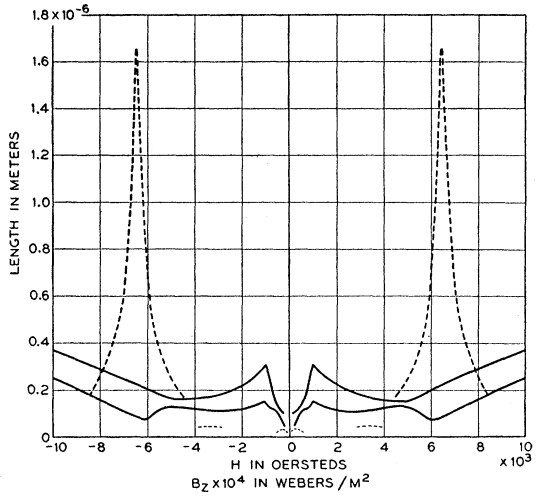

FIG. 17. Solid lines show $1/|k|$ *vs* magnetic field at 72 000 Mc/sec for the two waves which propagate normal to the surface (along a two-fold axis) in the pure bismuth sample for which results are shown in Fig. 3. The field range shown is less than in Fig. 3; at higher fields than those shown here, the $1/|k|$ values become much larger and conditions become quite classical. The dashed lines show the left-hand side of Eq. (B1). Where the dashed line is considerably above a solid line, anomalous skin effect conditions prevail.

relaxation time τ was obtained directly from the experimental results.

The results of such a calculation are presented for two cases in Figs. 17 and 18. Since the material is anisotropic, there are two waves in the material and therefore two values of $|k|^{-1}$, both of which are plotted in the range of magnetic fields in which they are smallest. Figure 17, which is relevant to the pure bismuth results shown in Fig. 3 for 72 000 Mc/sec, shows one of the most anomalous cases met in these

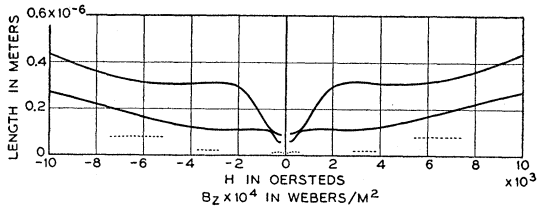

FIG. 18. Solid lines show skin depths *vs* magnetic field at 72 000 Mc/sec for the two waves which propagate normal to the surface (along a two-fold axis) in the alloy sample for which results are shown in Fig. 11. The dashed lines show the left-hand side of Eq. (B1). Since the dashed lines are at all fields well below the solid curves, classical skin effect conditions prevail at all points here. This is an alloy case in which impurity scattering has reduced the relaxation time τ.

experiments at this frequency. Even in this case, the clearly anomalous region is confined to the neighborhood of zero field and of the cyclotron resonance for holes. Figure 18 shows how alloying changes the factors in Eq. (B1) so that conditions are classical at all fields. This figure corresponds to results shown in Fig. 11 for 72 000 Mc/sec.

The region of the field in which anomalous conditions prevail at 72 000 Mc/sec is comparable in size for data taken with B_z along a three-fold axis in pure bismuth with that shown in Fig. 17. It is somewhat larger in the data at 24 000 Mc/sec in spite of the fact that $1/|k|$ is larger there, because the values of $\omega\tau$ are lower at that frequency.

We conclude from the results shown in Figs. 17 and 18 and from the fit obtained between the data and the classical theory that the anomalous skin effect does not occur over a sufficiently large fraction of the field range in these experiments for it to alter the shape of the curves in a vital way.